AD-A254 396

ATION PAGE

Form Approved
OBM No. 0704-0188

Pub
mai
for
the

1 hour per response, including the time for reviewing instructions, searching existing data sources, gathering and ation. Send comments regarding this burden or any other aspect of this collection of information, including suggestions formation Operations and Reports, 1215 Jefferson Davis Highway, Suite 1204, Arlington, VA 22202-4302, and to 9), Washington, DC 20503.

1. Agency Use Only (Leave blank).	2. Report Date. 1992	3. Report Type and Dates Covered. Final - Journal Article

4. Title and Subtitle.
Turbulent Transport from an Arctic Lead: A Large-Eddy Simulation

5. Funding Numbers.

Contract	
Program Element No.	0601153N
Project No.	03103
Task No.	380
Accession No.	DN251030
Work Unit No.	14411A

6. Author(s).
John W. Glendening and Stephen D. Burk

7. Performing Organization Name(s) and Address(es).
Naval Oceanographic and Atmospheric Research Laboratory
Atmospheric Directorate
Stennis Space Center, MS 39529-5004

8. Performing Organization Report Number.
JA 442:016:91

9. Sponsoring/Monitoring Agency Name(s) and Address(es).
Naval Oceanographic and Atmospheric Research Laboratory
Basic Research Management Office
Stennis Space Center, MS 39529-5004

10. Sponsoring/Monitoring Agency Report Number.
JA 442:016:91

11. Supplementary Notes.
Published in Boundary-Layer Meteorology
*Department of Meteorology, Naval Postgraduate School, Monterey, CA

12a. Distribution/Availability Statement.
Approved for public release; distribution is unlimited.

12b. Distribution Code

13. Abstract *(Maximum 200 words).*

The upward transfer of heat from ocean to atmosphere is examined for an Arctic "lead," a break in the Arctic ice which allows contact between the cold atmosphere and the relatively warm ocean. We employ a large-eddy model to compute explicitly the three-dimensional turbulent response of the atmosphere to a lead of 200 m width. The surface heat flux creates a turbulent "plume" of individual quasi-random eddies, not a continuous updraft, which penetrate into the stable atmosphere and transport heat upward.

Maximum updraft velocities and turbulence occur downwind of the lead rather than over the lead itself, because the development time of an individual thermal eddy is longer than its transit time across the lead. The affected vertical region, while shallow over the lead itself, grows to a height of 65 m at 600 m downwind of the lead; beyond that, the depth of the turbulent region decreases as the eddies weaken. The maximum vertical turbulent heat flux occurs at the downwind edge of the lead, beyond which a relative maximum extends upward into the plume. Negative surface heat flux immediately downwind of the lead creates a growing stable layer, but above that internal boundary layer the turbulent heat flux is still positive. Updraft maxima are typically 28 cm/s, but compensating downdrafts result in time-averaged vertical velocities of less than 1 cm/s in the plume. Conditional sampling separates the updraft and downdraft contributions. Formulas for the horizontal eddy development distance and for the vertical plume penetration height are presented. The relative importance of mean and turbulent transport is compared for both vertical and horizontal heat transfer; turbulence dominates the vertical heat transport whereas mean advection dominates the horizontal transport, these offsetting transports producing a quasi-stationary state.

14. Subject Terms.
Arctic leads, boundary layer, mesoscale

15. Number of Pages.
24

16. Price Code.

17. Security Classification of Report.	18. Security Classification of This Page.	19. Security Classification of Abstract.	20. Limitation of Abstract.
Unclassified	Unclassified	Unclassified	SAR

TURBULENT TRANSPORT FROM AN ARCTIC LEAD: A LARGE-EDDY SIMULATION

JOHN W. GLENDENING[1] and STEPHEN D. BURK[2]

[1]*Department of Meteorology, Naval Postgraduate School, Monterey, California, U.S.A.*; [2]*Naval Oceanographic and Atmospheric Research Laboratory, Atmospheric Directorate, Monterey, California, U.S.A.*

(Received in final form 4 October, 1991)

Abstract. The upward transfer of heat from ocean to atmosphere is examined for an Arctic "lead", a break in the Arctic ice which allows contact between the cold atmosphere and the relatively warm ocean. We employ a large-eddy model to compute explicitly the three-dimensional turbulent response of the atmosphere to a lead of 200 m width. The surface heat flux creates a turbulent "plume" of individual quasi-random eddies, not a continuous updraft, which penetrate into the stable atmosphere and transport heat upward.

Maximum updraft velocities and turbulence occur downwind of the lead rather than over the lead itself, because the development time of an individual thermal eddy is longer than its transit time across the lead. The affected vertical region, while shallow over the lead itself, grows to a height of 65 m at 600 m downwind of the lead; beyond that, the depth of the turbulent region decreases as the eddies weaken. The maximum vertical turbulent heat flux occurs at the downwind edge of the lead, beyond which a relative maximum extends upward into the plume. Negative surface heat flux immediately downwind of the lead creates a growing stable layer, but above that internal boundary layer the turbulent heat flux is still positive. Updraft maxima are typically 28 cm/s, but compensating downdrafts result in time-averaged vertical velocities of less than 1 cm/s in the plume. Conditional sampling separates the updraft and downdraft contributions. Formulas for the horizontal eddy development distance and for the vertical plume penetration height are presented. The relative importance of mean and turbulent transport is compared for both vertical and horizontal heat transfer: turbulence dominates the vertical heat transport whereas mean advection dominates the horizontal transport, these offsetting transports producing a quasi-stationary state.

1. Introduction

During the Arctic winter, pack ice separates the cold Arctic atmosphere from the relatively warm Arctic ocean. Breaks in the pack ice allow air-ocean contact, generating large upward fluxes of heat and moisture. The term "lead" usually refers to a transient break resulting from local ice stress divergence, whereas "polynya" usually refers to a semi-permanent break – typically much larger than a lead – associated with a specific location. Leads are approximately linear, with widths ranging from 1 m to 1 km and lengths from 1 km to 100 km. Air-ocean temperature differences are typically 20–40 °C, creating heat fluxes up to two orders of magnitude larger than those over the pack ice. Consequently the total heat input into the atmosphere from leads can be larger than that from the surrounding ice, despite the relatively small area coverage of the leads (Maykut, 1978). This heat release makes Arctic winters less frigid, at sea level, than those of the Antarctic (Smith *et al.*, 1990).

The influence of sea ice on the large-scale polar climate has been a subject of

Boundary-Layer Meteorology **59**: 315–339, 1992.

many modeling studies. Large-scale models have included a sea ice effect in different ways: with a specified surface boundary condition (North and Coakley, 1979), with parameterized sea ice in an ocean model (Wetherald and Manabe, 1981), and with a one-layer thermodynamic model (Washington and Meehl, 1984). Ledley (1988) specifically separated out the effect of leads in a coupled climate-sea ice model, finding a lead-temperature feedback that increased the annual zonally-averaged surface air temperature in the north polar region by 1.0 K when the winter lead fraction was increased from 1.1 to 4.3%. Since leads are small-scale features, their effects must be parameterized in large-scale models.

The small-scale physics of pack ice and leads has been reviewed by Untersteiner (1986). Smith *et al.* (1990) summarized several lead observational experiments, which primarily investigated the region over the lead itself. For example, Andreas *et al.* (1979) described heat flux variations with fetch over several leads and Smith *et al.* (1983) investigated larger polynyas for which the heat flux was not fetch-limited. Heat and momentum transfer coefficients for leads/polynyas have resulted (e.g., Andreas and Murphy, 1986). Aircraft observations have found plumes from Arctic leads extending up to 4 km vertically (Schnell *et al.*, 1989), indicating that such plumes can penetrate the Arctic inversion and transport heat into the lower troposphere.

Previous small-scale modeling of lead effects has been relatively limited and has considered only the response above the lead itself. Shreffler's (1975) two-dimensional model employed eddy diffusivity closure and a molecular surface sublayer to predict surface fluxes and vertical growth of the internal boundary layer (IBL) created over a 20 m wide lead. Lo (1986) employed a two-dimensional model with a turbulent kinetic energy (TKE) closure to predict profile variations as a function of downwind distance over a polynya.

This investigation primarily discusses the region of turbulence and upward heat flux which occurs downwind of the lead, rather than the region immediately above the lead, because the strongest turbulent response occurs in the downwind region. Also, this investigation considers lead effects in a strongly stratified upstream environment, as is typical of the Arctic, whereas both previous numerical models assumed the upstream environment to be neutrally stratified. Our approach is embodied in Figure 1, an observed downwind growth of individual eddies over a lead. We use a large-eddy (LE) model to simulate the thermal eddies created by a lead and thereby determine their integrated effect. We find that the strongest vertical turbulence and deepest upward heat transfer occurs downwind of the lead, rather than immediately above it, because an individual eddy's travel time over the lead is smaller – for our chosen lead width of 200 m – than its development time. The eddies therefore continue to grow downwind of the lead itself, creating an extensive turbulent "plume" with significant upward heat flux. (We shall use the term "plume" to refer to the region of time-averaged upward heat flux created by the lead as a result of individual eddy transports.)

A major field program to study Arctic leads and enhance understanding of

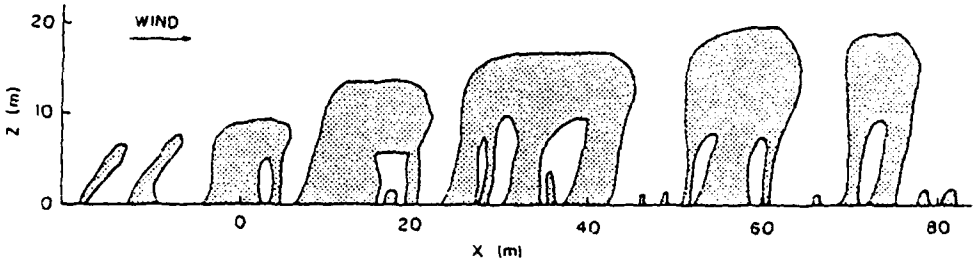

Fig. 1. Growth of eddies over a lead: stippling indicates individual thermals as interpreted from smoke plume photographs by Smith *et al.* (1983).

coupled atmosphere/ice/ocean dynamics, called LEADEX, will be conducted during Spring 1992. The effect of both single and multiple leads upon atmospheric and oceanic properties will be investigated. One motivation for the present study is to assist planning for instrumentation deployment around a lead.

2. Large-Eddy Model

The large-eddy (LE) model we employ is fundamentally that described by Moeng (1984), which uses a Deardorff K-theory parameterization for the sub-eddy scale closure. The inhomogeneous forcing created by the lead does require several model changes, since the existing coding assumed the surface forcing to be horizontally homogeneous. Surface values of temperature, temperature flux, and stress are allowed to vary in the x direction and the predicted mean variables become functions of x. In addition, the distinct differences between directions perpendicular and transverse to the lead require a rectangular grid to provide a long downwind domain.

The simulation must treat strongly stratified regions close to the surface adequately, though such is not the fundamental purpose of an LE model since no large eddies exist in such regions. To accomplish this, we modify the subgrid parameterization. First, the surface layer is allowed to be stable, using Monin–Obukhov similarity theory with relationships between surface profiles and fluxes given by Businger *et al.* (1971). Second, the subgrid mixing length scale l is not allowed to exceed the similarity value kz/ϕ_m in the surface layer (i.e., for $z < |L|$), where k is the von Karman constant, ϕ_m is the dimensionless wind shear, and L is the Monin–Obukhov length. Third, to retain congruence between the mixing coefficient parameterized in the model – i.e., $K_m = cle^{1/2}$, where e is the subgrid TKE and c is an empirical proportionality constant of 0.1 – and that of surface-layer similarity – i.e., $K_m = kzu_*/\phi_m$, where u_* is the surface friction velocity – the subgrid TKE is set to $(u_*/c)^2$ at the lowest grid point. Our subgrid parameterization assumes, for stable stratification in the surface layer, that vertical mixing dominates horizontal mixing and that the vertical mixing length is smaller than that set by the grid spacing.

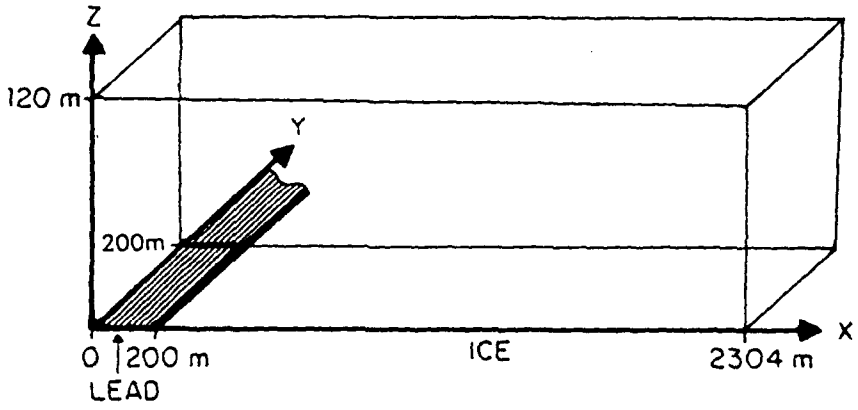

Fig. 2. Lead (water) and ice regions within the model domain.

A hydrostatic radiation boundary condition (Klemp and Durran, 1983) is employed at the model top. This condition does not eliminate reflections from the model top, since the model is non-hydrostatic, but it does reduce them: in one test generating a strong impulsive gravity wave, this radiation condition reduced vertical velocities resulting from trapped modes by 2/3. Lateral boundary conditions (BC) are cyclical, as the model is spectral. Cyclic BC are entirely appropriate in the lead-parallel direction. Cyclic BC in the lead-perpendicular direction would simulate a series of leads, rather than a single lead, if the model were to be run for a sufficiently long period; our simulation, however, is terminated before lead-induced effects can propagate through the domain and so represents a single lead. The model equations do not introduce artificial horizontal diffusion, but wavelengths smaller than $3\Delta x$ are filtered at every time step to control non-linear instability.

To reduce storage space requirements, the model is run without the complexities of water vapor, cloud formation, or radiative transfer. At cold Arctic temperatures, with small saturation vapor pressures, the latent heat flux from an open lead is typically 25% of the total heat flux (Andreas *et al.*, 1979); such latent heat fluxes can be significant if condensation occurs. Satellite observations have found both clear and cloudy regions extending downwind from leads (R. W. Fett, personal communication). The latent heat flux ceases when the lead freezes over, but the sensible heat flux through thin ice can still be significant.

3. Simulation Parameters

We simulate a single idealized lead in an Arctic ice pack. Our linear lead is 200 m wide and infinitely long, with a surface temperature of −2 °C. Figure 2 indicates the lead location within the model domain. The ice temperature is −29 °C, giving a surface temperature difference of 27 °C between water and ice. For our base-state atmosphere, constant throughout the domain, we choose a strongly stable

stratification $\partial\theta/\partial z = 10$ K/km with $\theta = -27$ °C at the surface. The geostrophic wind is perpendicular to the lead at 2.5 m/s. The ice is slightly rougher ($z_0 = 0.1$ cm) than the water in the lead ($z_0 = 0.01$ cm). The Coriolis parameter represents a latitude of 79° N.

The scales of interest in this simulation are small by typical convective large-eddy standards. Our grid spacing is 4 m vertically and 8 m horizontally. The domain extends 2304 m perpendicular to the lead (in the x direction), 200 m transversely and 120 m vertically. The lead-perpendicular domain must be extensive to avoid cyclic BC interference; array size maxima therefore force a limited lead-parallel domain, but the latter is large enough to allow vortex roll formation. An empirically-determined time step of 0.5 s is required for numerical stability with the small grid spacing employed.

The model is initialized in a horizontally homogeneous state, the initial temperature being that of the base state. The initial wind is the model's one-dimensional equilibrium solution over the ice surface, so the flow would be quasi-stationary if no lead were present. Due to the stable stratification, initially all TKE is subgrid and no large eddies exist except for specified random velocity perturbations of 0.01 m/s in the lowest layer. This initialization creates a transient, since effectively the lead "opens" instantaneously rather than over several hours. The initialization procedure was largely dictated by computer time constraints: it eliminates the time scale associated with the lead opening.

Since turbulent fields are simulated, the results must be averaged. Unless otherwise indicated, all mean results presented are spatially averaged in the lead-parallel direction and time averaged over a period from 576 s to 702 s after model initialization, when the region from the upwind lead edge to 800 m downwind of the lead has achieved quasi-stationarity. Each average represents 6048 individual values.

4. Simulation Results

4.a. Quasi-stationarity

The instantaneous opening of the lead creates an initial transient, as heat is released into the air above the lead, which increases in depth and strength until advection of cold air balances the heat transfer. After the transient propagates downwind, a quasi-stationary state is approached. Figure 3 depicts passage of the initial transient for $x = 500$ m and $x = 1000$ m; the indicated values are for a height of 32 m, averaged over 36 s and in the y direction. At a given location, the transient first appears as a negative vertical velocity (w), with the subsequent positive velocity relaxing towards a mean vertical velocity typically less than 1 cm/s. Simultaneously, potential temperature (θ) increases rapidly from its initial state and then relaxes toward a quasi-stationary solution. Based upon analysis of the temporal adjustment of w and θ, and mean w contours given in the next section, we consider

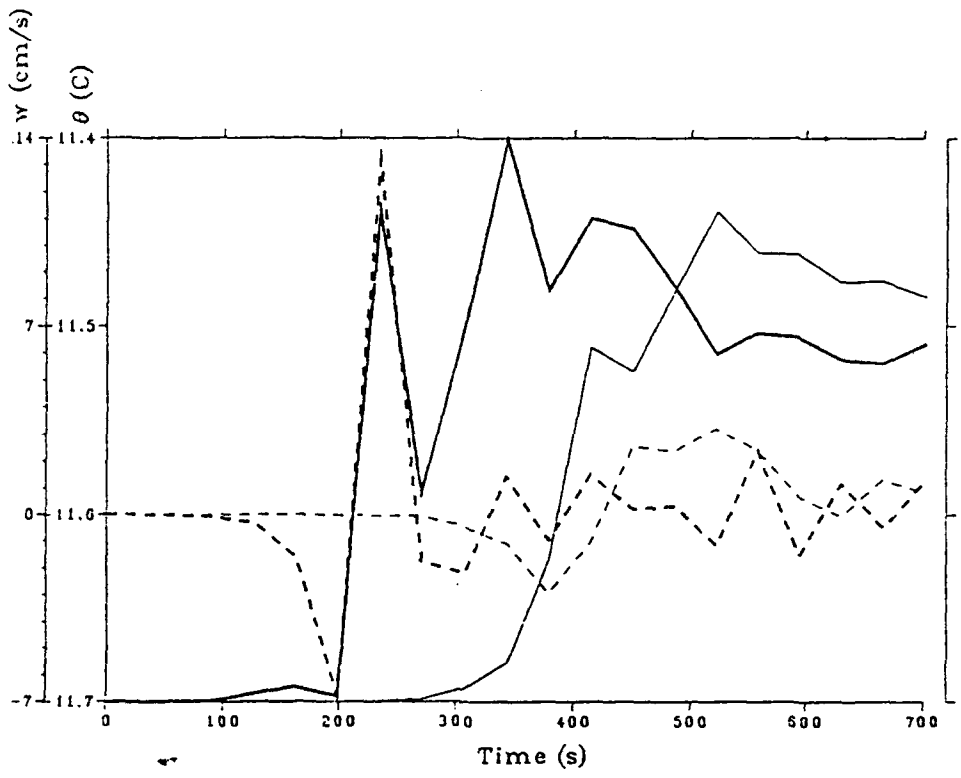

Fig. 3. Potential temperature (solid) and vertical velocity (dashed) changes as a function of time at $x = 500$ m (heavy) and $x = 1000$ m (thin).

$x = 1000$ m to be the downwind limit of quasi-stationarity for our chosen time-averaging period. This does mean that large changes are occurring for $x > 1000$ m: near the center transient, at $x = 1400$ m over the simulation period 576 to 702 s, the maximum $\partial\theta/\partial t$ is only 1×10^{-3} K/s. Heat transfer essentially occurs within $x < 1000$ m for both the transient and the quasi-stationary events.

4.b. Individual eddy structure

We first examine the individual eddy structure. Since eddies continually grow and decay, the variables at any given point continually change with time. Near the upwind edge of the lead, the turbulent scales are too small to be resolved by the finite grid, but the eddies become resolved as they grow downwind. Maximum turbulence occurs downwind of the lead itself, as discussed in Section 5b. Figure 4 depicts instantaneous vertical velocities over the region of maximum eddy growth at 648 s after model initialization, the middle of the averaging period. Two levels are shown; for clarity, only a partial domain is displayed. At the lower level ($z = 24$ m), upward velocities are largest nearer the lead, where they exhibit linear features parallel to the wind – suggestive of roll vortex formation – with an along-wind/cross-wind aspect ratio greater than one; farther downwind the eddies are

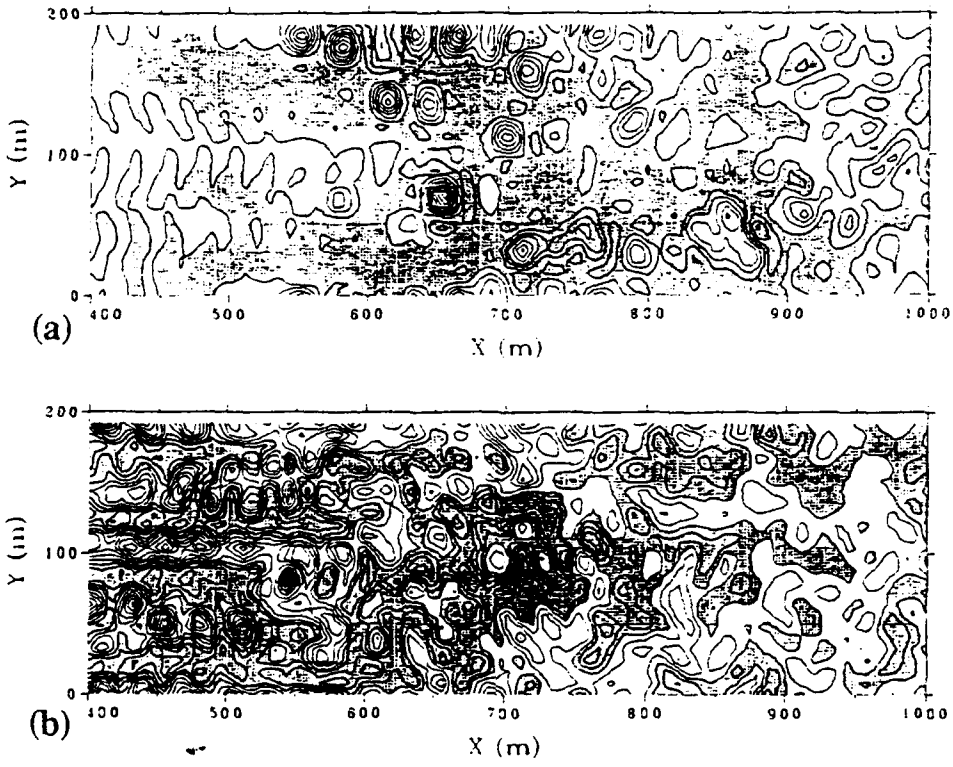

Fig. 4. Instantaneous vertical velocity at t = 648 s for (a) z = 56 m, (b) z = 24 m. Contours of 10 cm/s; shading indicates downward motion.

less intense, lose their linear structure, and eventually decay due to the lack of upward surface heat flux. At the upper level (z = 56 m), upward velocities are negligible close to the lead because the eddies have not yet penetrated to that depth, the first eddies to do so being hot columns with large upward velocities and small lateral extent; farther downwind, the eddies become larger in extent with smaller upward velocities.

Figure 5 illustrates the tendency for the eddies to orient themselves in an along-wind direction, i.e., to have an aspect ratio greater than one. Vertical velocities in the along-wind and cross-wind directions at a height of 40 m have been averaged based upon their relative distance from the local updraft maxima; thus Figure 5 represents perpendicular slices through a "typical" updraft. Averaged over the entire domain, the along-wind extent is double the cross-wind extent; Figure 4 indicates that this aspect ratio is actually a decreasing function of downwind distance. Since the transverse width of a typical updraft is significantly smaller than half the transverse domain, the lateral cyclic boundary conditions do not artificially limit the eddy size.

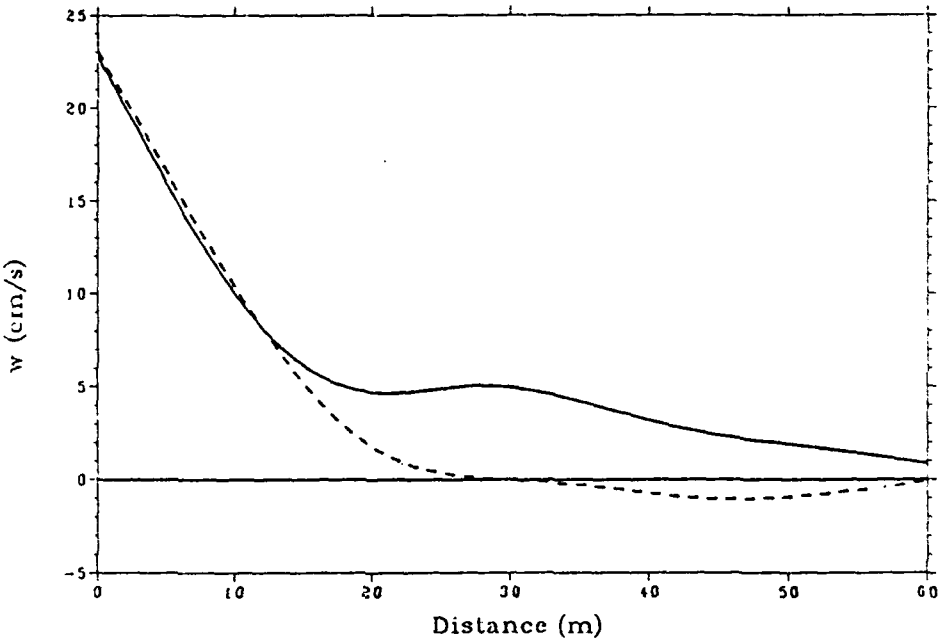

Fig. 5. Vertical velocity as function of distance from the local updraft maximum in along-wind (solid) and cross-wind (dotted) directions at z = 40 m and t = 648 s.

4.c. Mean vertical velocities

Figure 6 depicts mean vertical velocities over the entire model domain. The initial transient created by the instantaneous lead opening is apparent for $x > 1000$ m (parcels initially over the lead have advected to between x = 1600–1800 m at the middle of the averaging period). The vertical velocity contours tilt with height near the upper boundary due to the radiation BC applied there; if trapped modes were prominent, these contours would be vertically oriented.

In the quasi-stationary region, from $x = 0$ to $x = 1000$ m, mean vertical velocities are small – typically less than 1 cm/s – because the large upward velocities of the individual eddy updrafts – with typical maxima of 28 cm/s – are compensated by eddy downdrafts. These small mean vertical velocities are a consequence of the small eddy travel time over the lead; significantly larger mean vertical velocities would be expected over much wider leads or for winds more parallel to the lead. The downward velocity near x = 50 m reflects the near-surface speedup of the lead-perpendicular component of the wind, which is created by downward mixing of higher momentum air and by the smaller z_0 of the water.

4.d. Mean turbulence

Near the surface, turbulent length scales are smaller than the model resolution so all turbulent kinetic energy (TKE) is subgrid. Figure 7a depicts this subgrid energy, which increases in magnitude and vertical extent with distance over the lead as

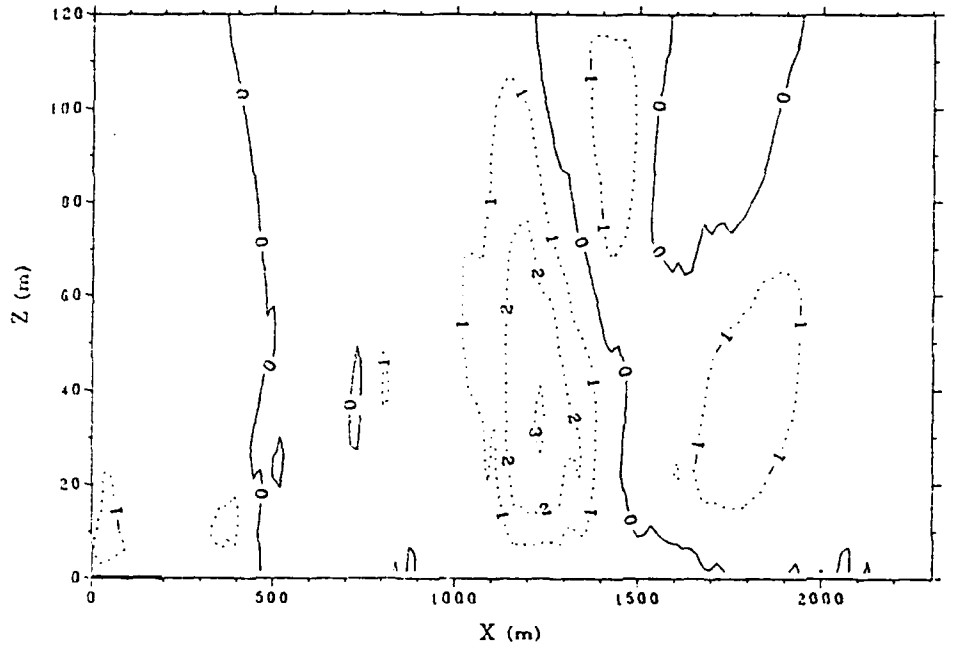

Fig. 6. Mean vertical velocity (in cm/s).

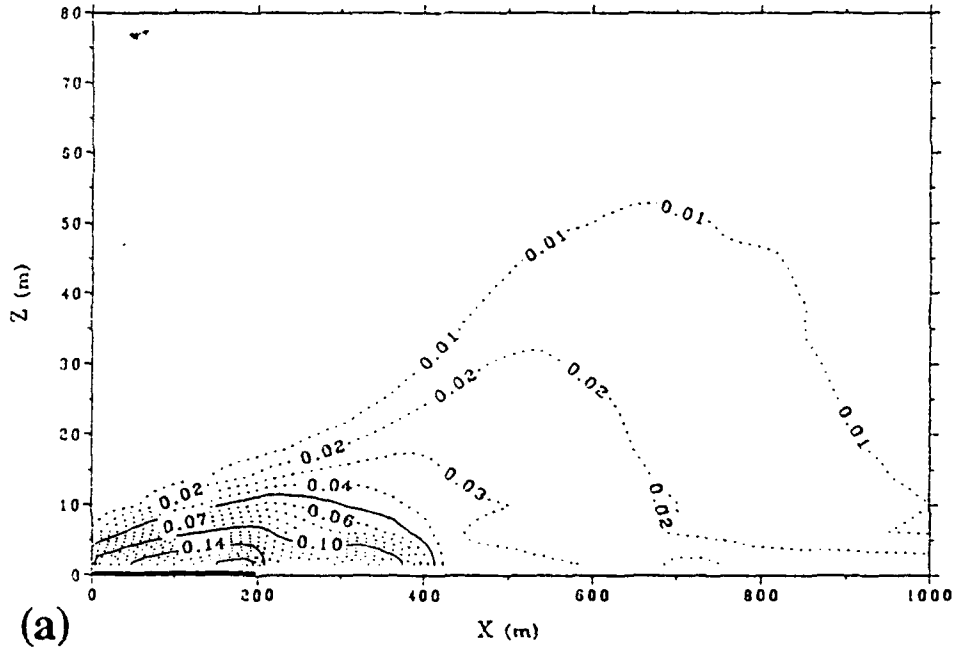

Fig. 7. (a) Mean subgrid turbulent kinetic energy (b) Mean resolved vertical turbulence ($\overline{w'^2}$); (c) Mean resolved horizontal turbulence ($\overline{u'^2} + \overline{v'^2}$); (d) Mean total turbulent kinetic energy (in m^2/s^2).

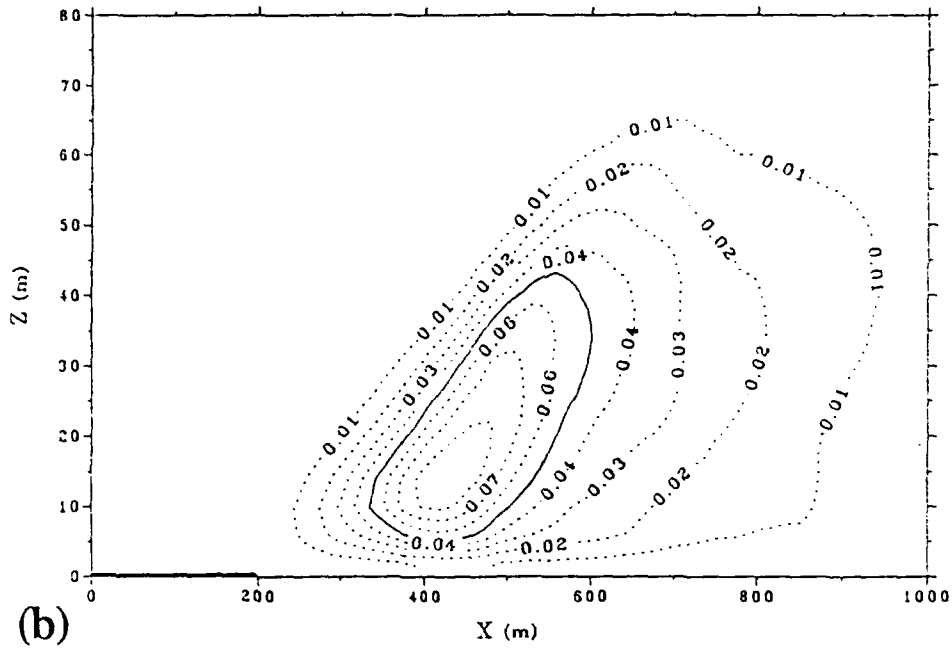

(b)

Fig. 7(b).

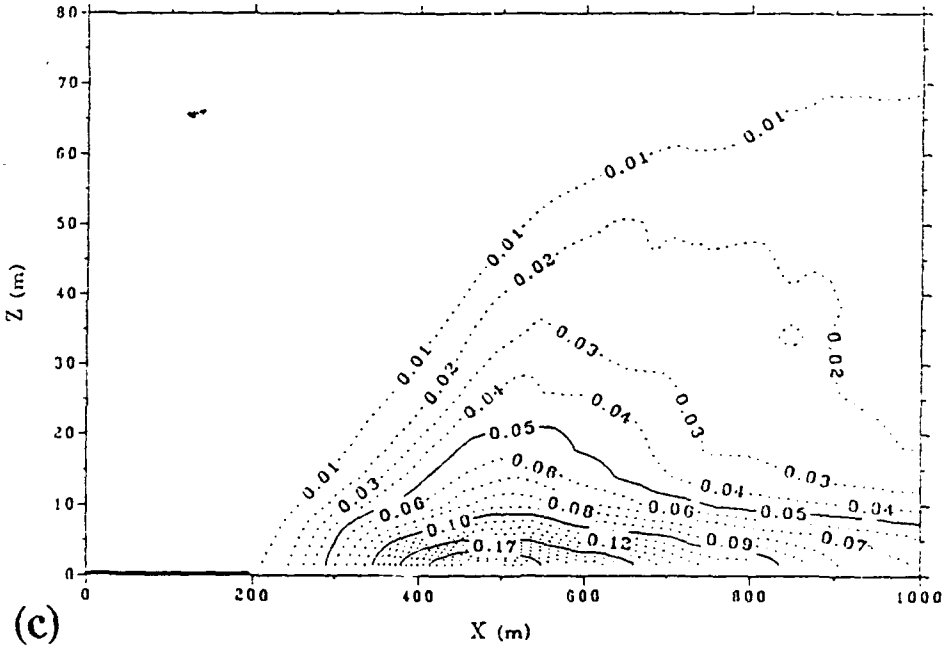

(c)

Fig. 7(c).

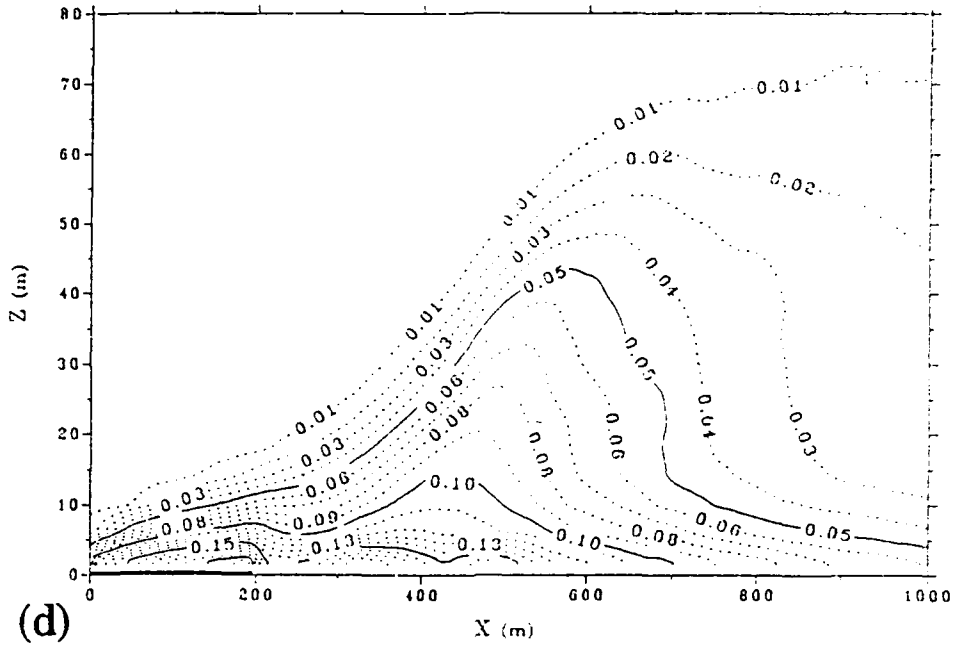

Fig. 7(d).

buoyant energy enters the atmosphere. The subgrid energy decays after losing contact with the buoyancy source, so its maximum occurs at the downwind edge of the lead.

As eddies move downwind, they grow in size and become resolved. Figure 7b depicts the resolved vertical turbulence, $\overline{w'^2}$, illustrating the strength and spatial extent of those eddies. The maximum $\overline{w'^2}$ occurs at x = 430 m, which corresponds to the position of maximum w for a typical individual eddy. Resolved horizontal turbulence (Figure 7c), resulting from horizontal flow to and from the vertical eddy structure, is largest at the surface.

The plume created by the lead is most evident in the total (i.e., resolved plus subgrid) TKE of Figure 7d, showing the maximum TKE tilting downstream with height. This turbulent plume is responsible for the heat transfer from lead to atmosphere. The turbulence extends upward to 70 m at x = 700 m, the maximum height of a typical eddy.

Because the resolved turbulence is created while growing into a strongly stratified region, the ratio of unresolved (i.e., subgrid scale) to total turbulence is large compared with that of convective LE simulations. This ratio is 0.24 at the turbulence maximum, which is small enough to allow eddy formation, and becomes smaller/larger in the turbulent region above/below that level.

4.e. Mean potential temperature

Figure 8 depicts mean potential temperatures. The upstream temperature profile is evident at x = 0 m, with the plume growing into the stably stratified region over

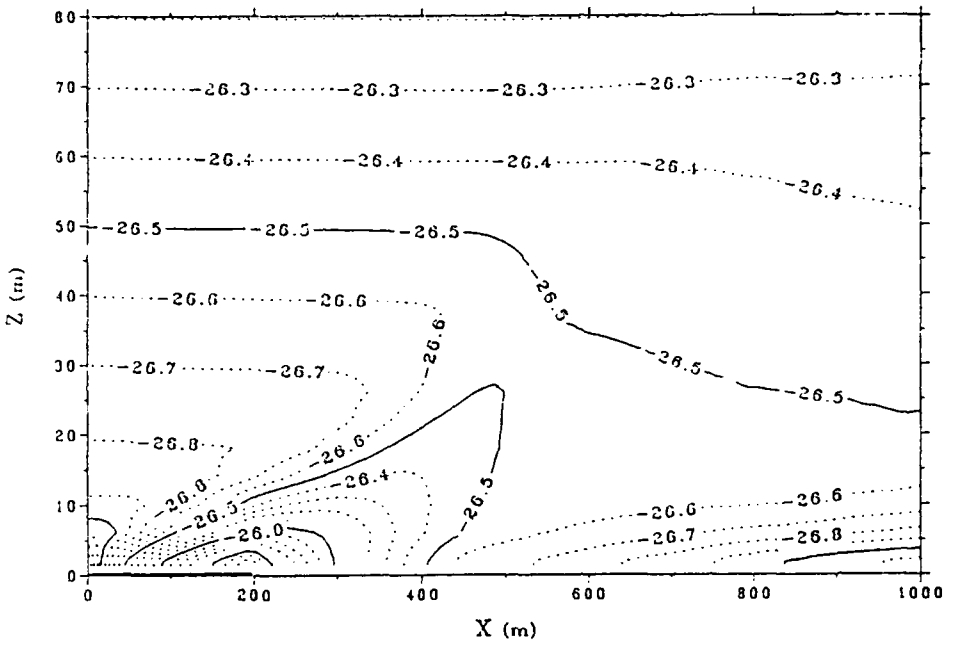

Fig. 8. Mean potential temperature (in °C).

the lead. The surface stratification is unstable over the lead and stable downwind of the lead. The stable IBL downwind of the lead is initially thin and poorly resolved but grows vertically as the eddies weaken and is apparent at $x \approx 300$ m.

Figure 9 gives the temperature change created by the lead, relative to temperatures upwind of the lead. The heat transferred to higher levels by turbulent eddies is primarily responsible for these changes; however, mean vertical velocities also make a contribution, as evidenced by the position of the zero contour which is affected by subsidence over the lead. The temperature increase is largest at the downwind edge of the lead. The growth in the vertical extent of temperature change, which ultimately reaches a depth of 65 m, is similar to the growth of the turbulent plume of Figure 7d.

4.f. Mean horizontal wind speed

The horizontal wind nearly parallels the x axis, due to the relatively low surface roughness of both ice and water. In consequence of this small surface roughness and the momentum transfer by eddy mixing, wind shear and shear production of TKE are small within the plume. The wind speed (and the lead-perpendicular wind component) increase over the lead due to lowered surface roughness and an increase in downward momentum transfer, creating the region of mean downward motion over the lead noted in Figure 6.

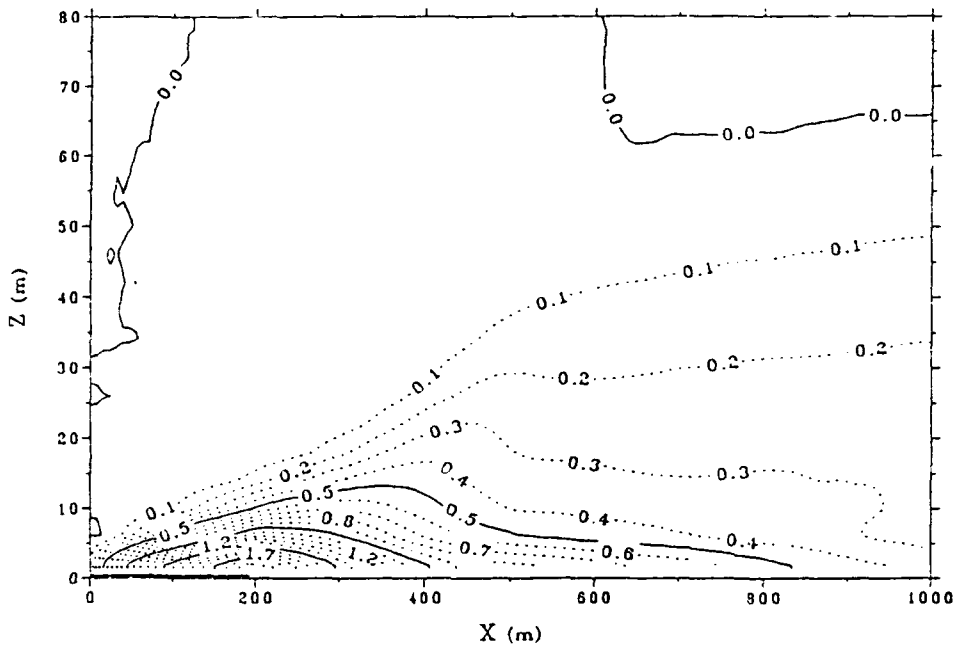

Fig. 9. Mean potential temperature change from upwind profile (in °C).

4.g. Mean turbulent temperature flux

Figure 10 gives the total (resolved plus subgrid) turbulent vertical temperature flux. Because the surface layer is not well resolved, the surface heat flux obtained from the surface-layer parameterization is not expected to be accurate in detail, but is instead considered a boundary condition driving the eddies and their associated heat transfer. Nevertheless, the effective surface heat transfer coefficient over the lead is 2.9×10^{-3}, close to the 2.4×10^{-3} value predicted by the observational fit of Andreas and Murphy (1986). We also note that the depth of the IBL at the downwind edge of the lead is around 20 m, in rough agreement with the 15 m value predicted for a lead by the formula of Schnell *et al.* (1989). At the surface, an increase in temperature flux with downwind distance results from instability-enhanced mixing overcoming the decreasing surface temperature contrast; Lo (1986) found this to occur for $x > 10^5 z_0$. Over the lead, the surface heat flux increases from 0.15 km/s to its absolute maximum of 0.18 km/s at the downwind edge of the lead, with a relative maximum extending downwind at higher levels into the plume.

Above the surface, positive heat transfer extends up to 60 m at $x = 550$ m. Note that significant upward temperature flux occurs above the re-established stably stratified IBL downwind of the lead. Negative temperature flux is not significant at the top of the plume, where the thermals grow into the stably stratified base-state atmosphere; this is unlike a convective boundary layer (CBL) over a homogeneous

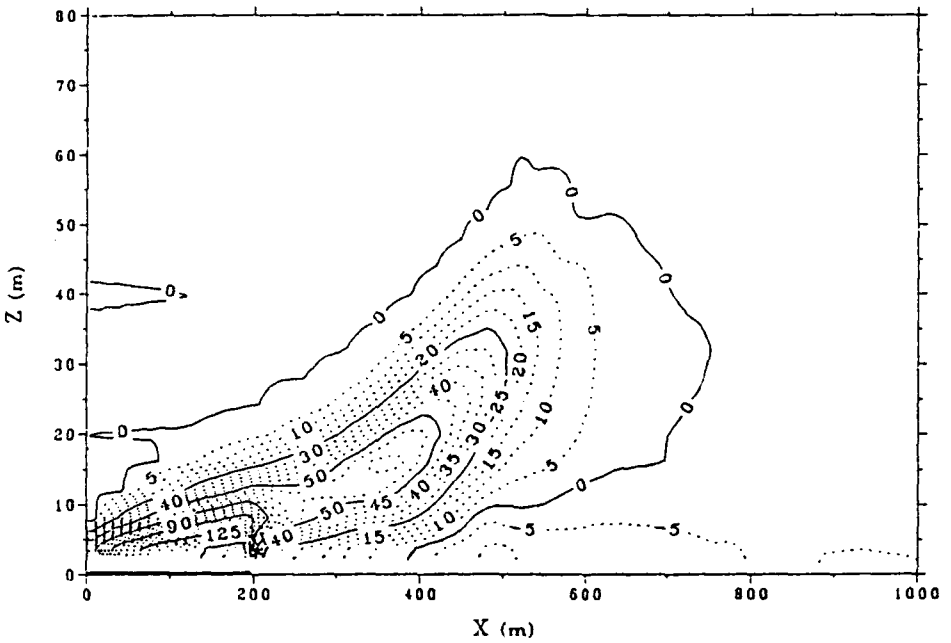

Fig. 10. Mean total vertical turbulent temperature flux (in $\times 10^{-3}$ Km/s).

surface, but must be interpreted cautiously since model resolution of the transition layer between buoyant and stable regions is only marginal. A tendency for the resolved and subgrid turbulent heat temperature flux solutions to separate is evidenced by a closed contour around the secondary maximum at $x, z = 360$ m, 16 m.

Eddy processes can produce upward temperature fluxes in stably stratified regions. Such counter-gradient fluxes occur around the plume perimeter. Figure 11 outlines the region of countergradient temperature flux with a heavy dashed line, the region essentially being that where $0 < \overline{w'\theta'} < 20$ Km/s. This counter-gradient flux is produced solely through the action of the large eddies, since the subgrid flux is required to be down-gradient. The counter-gradient temperature flux along the upper region of the growing plume is similar to the counter-gradient temperature flux found in the upper part of a CBL above a homogeneous surface, in which buoyant eddies rise into stably stratified air created by the surrounding subsiding air. We speculate that the lower region of counter-gradient temperature flux, which occurs where the growing stable IBL acts to increase the stable stratification, results from relatively warm air advected by eddies into a downwind region where it is buoyant and rises, thereby creating an upward temperature flux despite the mean stable stratification.

4.h. Comparison of mean and turbulent components of net heat transport

Horizontal turbulent transfer of heat is often assumed to be negligible, but such might not be true near a lead, where surface horizontal temperature gradients are

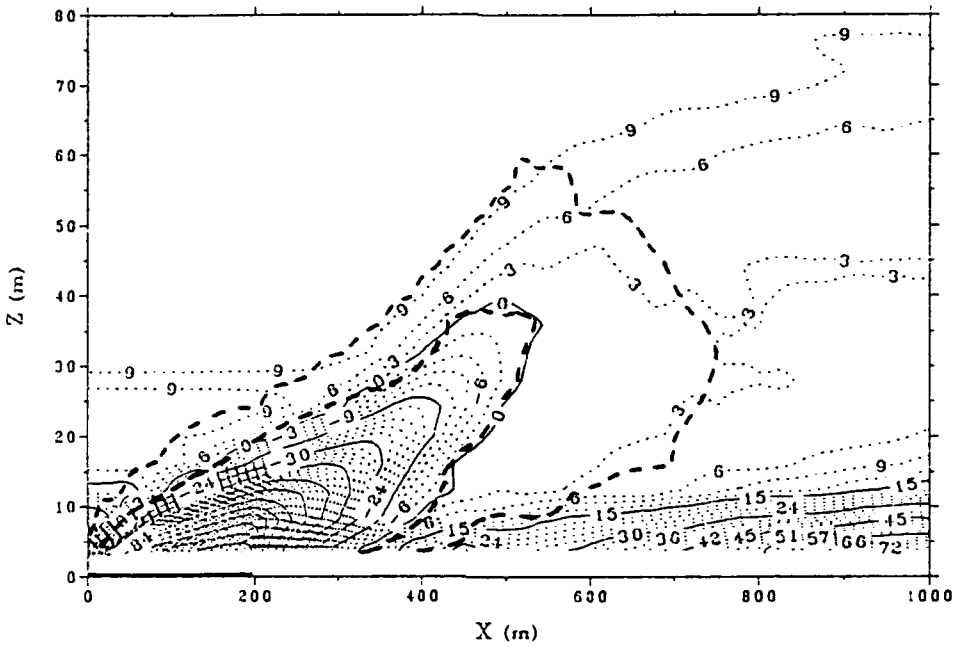

Fig. 11. $\partial\theta/\partial z$ (in K/km) with region of counter-gradient vertical temperature outlined by heavy dashed line.

very large. A LE model is unique in its ability to resolve such horizontal transfer, so partitioned heat fluxes are computed.

Both the vertical and horizontal net heat transport are partitioned into their mean and turbulent components, which are the advective and turbulent flux divergence contributions to $\partial\theta/\partial t$. This partitioning indicates that the vertical net heat transport is dominated by its turbulent component (Figure 12), as might be expected given the small mean vertical velocities. Vertical advection is significant only immediately over the lead, where the mean $\partial\theta/\partial z$ is very large. The horizontal net heat transport is, in contrast, almost entirely due to its mean advective component, the maximum turbulent component over the domain being 0.5×10^{-3} K/s at the upwind edge of the lead. Although the time-averaged horizontal turbulent transfer is small, a more detailed analysis indicates that the transfer associated with individual eddies, $-\partial\overline{u'\theta'}/\partial x$, is large but counteracting from one eddy to another.

Over the lead and in the upper portion of the downwind plume, heating resulting from the vertical divergence of the turbulent temperature flux is essentially balanced by cooling resulting from the horizontal advection of colder air upwind of the lead. Downwind of the lead at the surface and in the lower portion of the plume, heating resulting from the horizontal advection of air warmed by the lead is essentially balanced by cooling resulting from the vertical divergence of temperature flux. The result is a quasi-stationary temperature field.

One implication of the above is that simulating an Arctic lead with any model

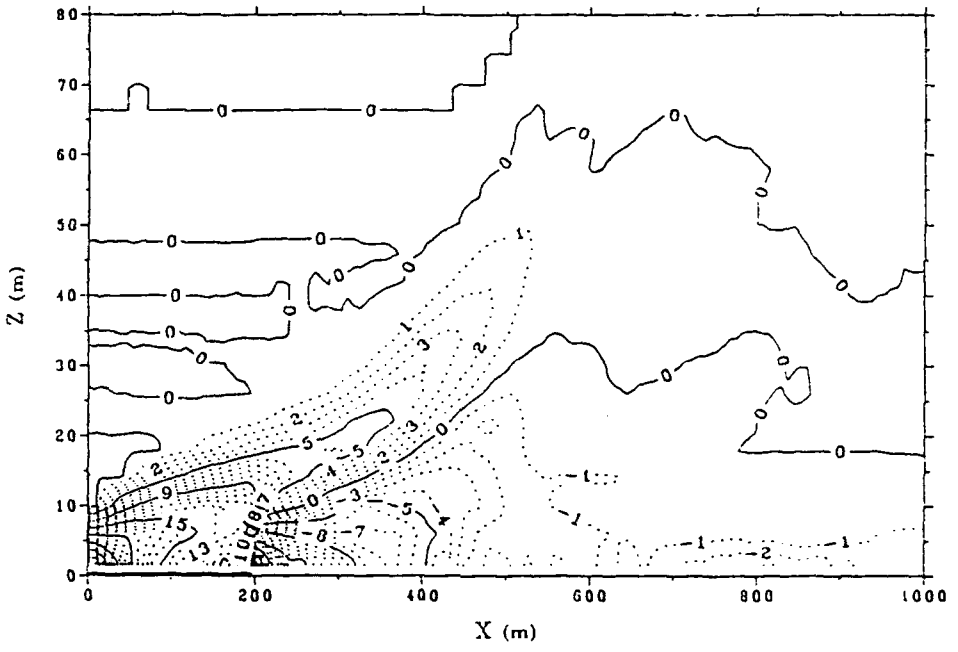

Fig. 12. Mean net vertical turbulent transport of heat (in $\times 10^{-3}$ K/s).

which requires a large artificial horizontal diffusivity for numerical stability would give inaccurate results, since the large horizontal mean temperature gradients would generate artificially large horizontal diffusion terms, which would in turn decrease the predicted turbulent vertical heat transport.

4.i. Conditional sampling

To investigate the turbulent eddy transport in greater detail, updraft and downdraft contributions are individually examined through conditional sampling, with variables being separately averaged based on the sign of the vertical velocity. This is useful only where the turbulent eddies are well resolved, i.e., downwind of the lead.

Figure 13 depicts conditionally-averaged vertical velocities for the resolved updrafts and downdrafts. The strongest updrafts occur near $x \approx 500$ m, with typical maximum velocities of 28 cm/s at a height of 30 m; significant upward motion extends to above 80 m. Compensating downdrafts are somewhat smaller in magnitude, their maximum vertical motion occurring nearer the surface than that of the updrafts.

Note that these contours represent a weighted sum over all eddies and are not representative of an individual eddy. For example, the axis tilt in Figure 13a is not indicative of individual updrafts – which are nearly vertically oriented due to the small wind shear – but instead indicates that the later an individual updraft reaches its maximum vertical velocity, the farther it is likely to be from both the

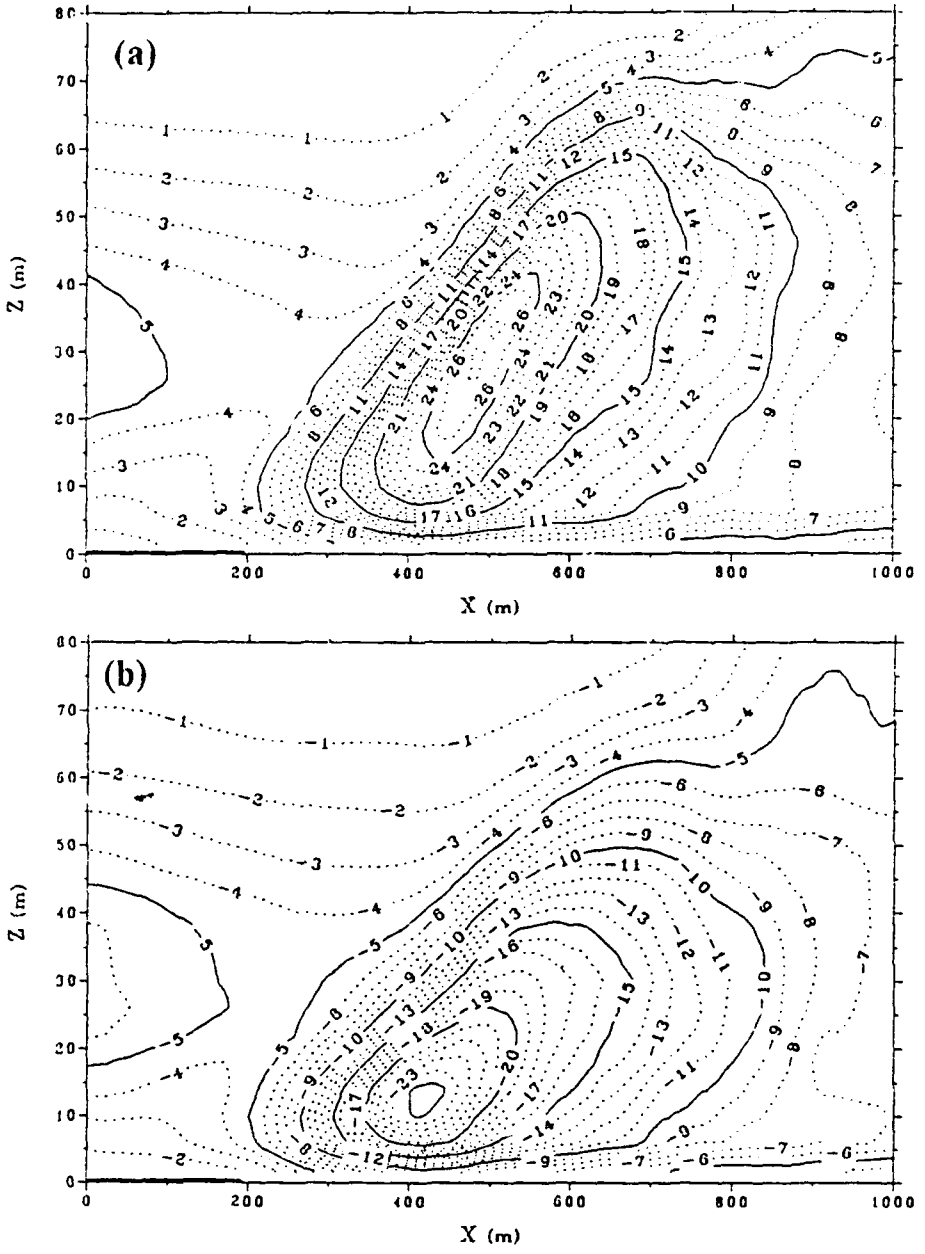

Fig. 13. Conditionally-averaged vertical velocity (in cm/s): (a) Upward motion; (b) Downward motion.

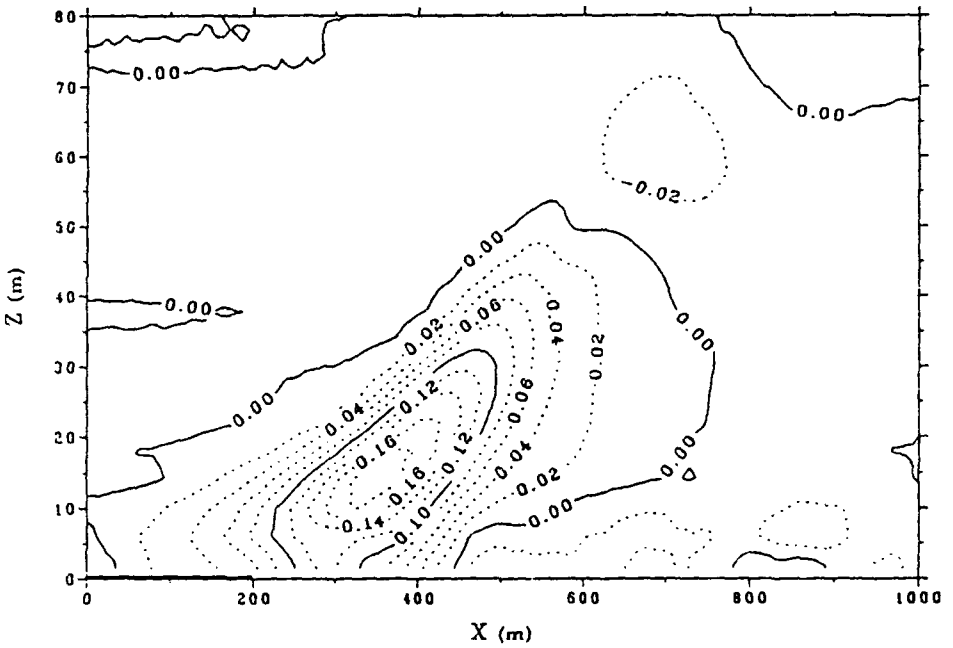

Fig. 14. Conditionally-averaged deviation of updraft potential temperature from mean potential temperature (in °C).

lead and the ground. The spacing of the contours results both from the variation between individual updrafts and from the along-wind width of the individual updrafts, the latter being typically 120 m (see Figure 5).

The difference between the conditionally-averaged updraft temperature and the mean temperature, which indicates updraft buoyancy, is shown in Figure 14. This temperature difference is largest near $x = 350$ m, so the position of maximum buoyant acceleration of an individual updraft is typically 150 m closer to the lead than that of its maximum vertical velocity. The negative buoyancy near $x, z = 700$ m, 62 m indicates buoyant overshooting and vertical motion induced in the stably-stratified atmosphere by penetrating eddies. The absence of significant negative buoyancy along the top of the developing plume – which is associated with the small downward heat flux there – contrasts with that over a homogeneous surface, for which downward heat flux is significant in updrafts at the top of a growing CBL (Wilczak and Businger, 1983). This minimal negative buoyancy likely results from horizontal motion under horizontally inhomogeneous conditions: an eddy advected into a region where the mean environmental temperature increases horizontally – as is true near the top of the developing plume downwind of the lead – will experience a decrease in buoyancy resulting from that horizontal motion and therefore penetrates less deeply into the stable region.

Figure 15 depicts the fractional time of upward motion. Since mean vertical

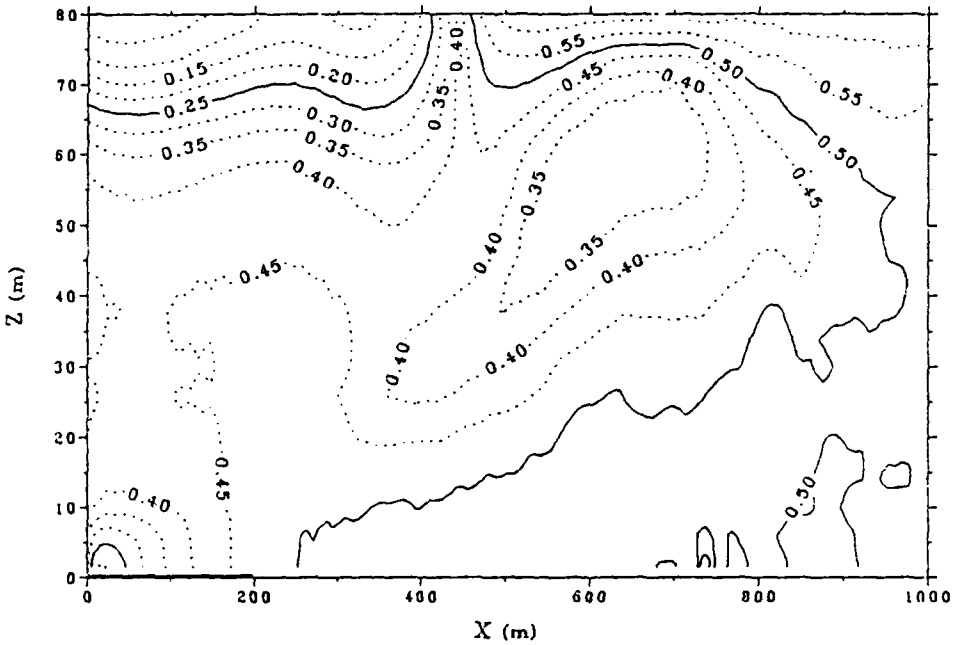

Fig. 15. Fractional time of upward motion.

velocities are small, conservation of mass requires that updraft velocities be larger than downdraft velocities when the fractional updraft occurrence is less than 0.5; this occurs over most of the domain, notably in the upper part of the plume.

Spatial differences in resolved vertical turbulence between the updrafts and downdrafts (not shown) are qualitatively similar to those of the conditionally-averaged vertical velocity, as might be expected. Updrafts contribute significantly more to the total $\overline{w'^2}$, than downdrafts do.

Figure 16 indicates that the maximum turbulent heat transports of the updrafts and downdrafts are comparable. However, the spatially-integrated turbulent heat transport of the updrafts is significantly larger than that of the downdrafts, demonstrating that the fundamental response of the atmosphere to the warm surface is to create buoyant updrafts to carry heat upward, whereas the downdrafts are a consequent induced response.

Updrafts transport heat upward via rising warm air, whereas downdrafts transport heat upward via sinking cold air. Both motions are thermally direct. A separate analysis finds that thermally indirect motion (e.g., rising cold air) can occur in individual eddies, but its occurrence is relatively infrequent. This is also evidenced by the small values of updraft negative buoyancy in Figure 14, temperatures in updrafts being almost always warmer than the time-average temperature at the same point.

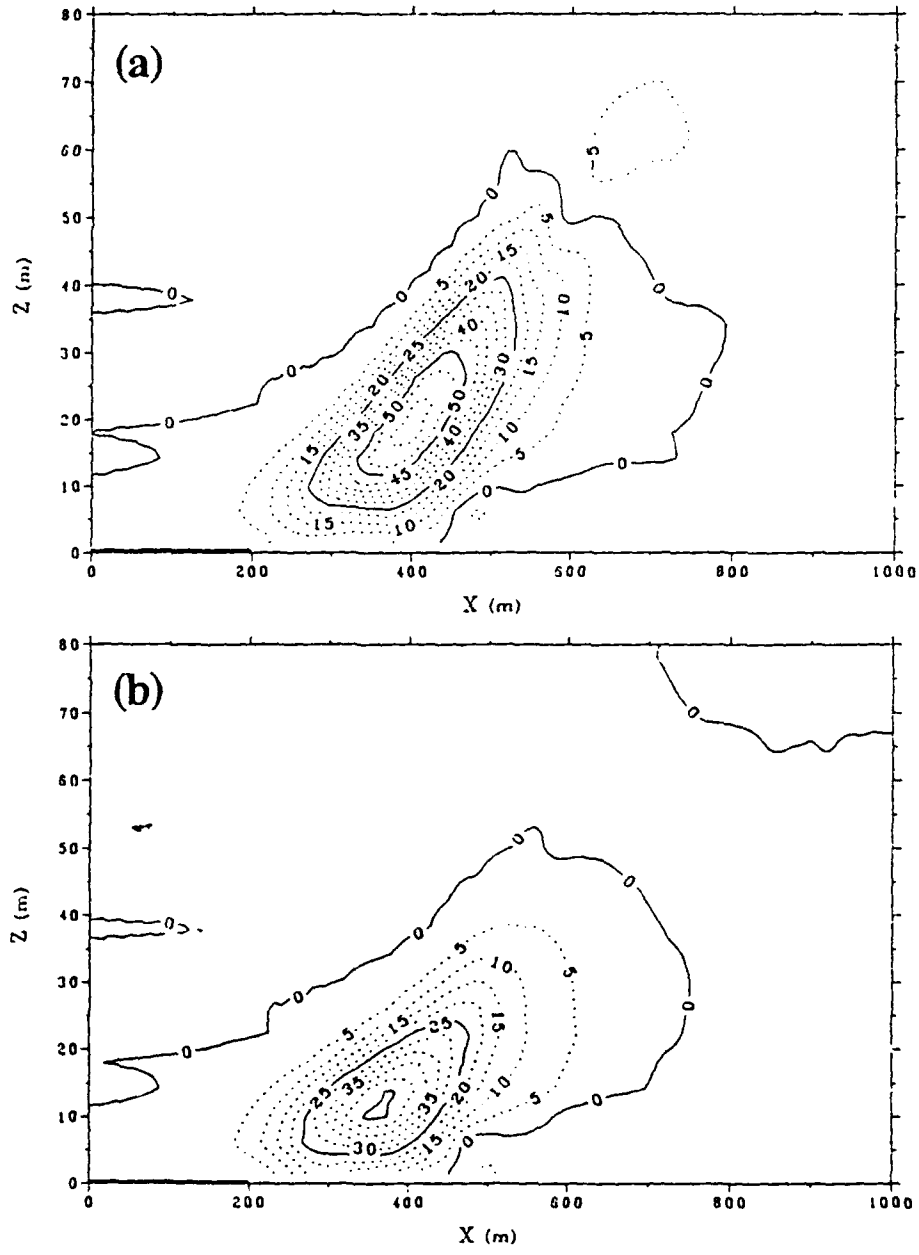

Fig. 16. Conditionally-averaged vertical turbulent temperature flux ($\overline{w'\theta'}$) (in $\times 10^{-3}$ Km/s): (a) Upward motion; (b) Downward motion.

5. Discussion

5.a. Physical interpretation

Over the lead, thermal eddies are initiated by the warm surface. This buoyancy input creates thermal updrafts, which accelerate vertically until their excess buoyancy is lost, overshooting into the stable stratification capping the boundary layer and eventually sinking back to become part of a downdraft. For our 200 m wide lead and 2.5 m/s lead-perpendicular wind, maximum thermal buoyancy typically occurs 150 m downwind of the lead with maximum upward velocity occurring 150 m farther downwind. Induced downdrafts accelerate downward until they are slowed by vertical pressure gradient forces created by the surface impermeability, at which time they spread horizontally; this accounts for the level of maximum vertical velocity of the downdrafts occurring closer to the ground than that of the updrafts.

Initially the thermals are small in vertical extent and their horizontal extent is correspondingly limited. Eddy growth and consolidation occur downwind, increasing both the vertical and horizontal extent of the eddies and creating a growing IBL. Growth and consolidation continue until the thermal structure disintegrates. Using smoke released at the upwind edge of a polynya to visualize the eddies (Figure 1), Smith *et al.* (1983) observed that "rising plumes of warm, moist air have a spacing approximately equal to the height at which they are observed: with increasing height the plumes tend to consolidate into fewer, larger plumes" (note that they use the word 'plume' to refer to an individual thermal, not – as is our usage – to refer to a turbulent region with a time-averaged upward heat flux).

5.b. Thermal development distance

For thermal eddies to develop primarily over the lead itself, hence for maximum turbulence to occur over a lead or near its downwind edge, their transit time over the lead should be longer than their development time. If a lead is sufficiently narrow that a thermal does not have time to develop fully while passing over it, growth and consolidation will continue downwind of the lead despite the absence of a surface buoyancy input. The maximum TKE at upper levels then occurs downwind of the lead rather than over it. For example, in Figure 13 the maximum updraft velocity typically occurs near $x = 500$ m, so it takes around 200 s for an updraft to reach maximum development, which is longer than its 80 s transit time across the lead.

A criterion for the horizontal development distance can be obtained from dimensional arguments. The thermal development time in a stratified environment scales with N^{-1}, where N is the Brunt–Väisällä frequency. From linear parcel theory, the time for an initially motionless disturbed parcel to reach maximum upward velocity is $(\pi/2)N^{-1}$ if there is no entrainment, but entrainment acts to increase the proportionality constant. Our results indicate that this time is approximately $4N^{-1}$. The maximum lead transit time is $S/|V|$, where S is the slant distance across

the lead in the wind-parallel direction and $|V|$ is the wind speed, so we propose the following criterion for turbulent development to occur primarily over the lead itself:

$$S > 4|V|N^{-1}, \tag{1}$$

where N is based upon $\partial\theta/\partial z$ upwind of the lead. Since $S/|V| = W/U$, where W is the lead width and U is the velocity component perpendicular to the lead, (1) is also a criterion for the lead width required for turbulence to develop over the lead itself: $W > 4UN^{-1}$.

For the strong stratifications and wind speeds typical of the Arctic, the required lead width is of the order of 1 km when the wind is perpendicular to the lead. This is much wider than is usual for leads in the central pack ice, so maximum turbulence should develop downwind of such leads unless the wind direction nearly parallels the lead. In contrast, polynya widths are often of the order of 1 km, so the development likely occurs above the polynya itself.

Equation (1) may be viewed as a comparison of two horizontal length scales, that of surface forcing and that of atmospheric response. The relative size of these length scales affects the qualitative nature of the turbulent field created by a lead and the magnitude of the mean vertical velocity.

5.c. Plume penetration depth

The depth of the plume created by a lead, and also the height to which individual thermals eventually rise, may be estimated by assuming that the buoyancy generated by passage over the lead creates a "bent-over plume", for which the initial vertical momentum is zero, rising into a stable environment. For such a case, Turner (1973, Equation 6.4.9) uses dimensional arguments to obtain a plume penetration depth Z_p:

$$Z_p \propto \left[\frac{F}{N^2}\right]^{1/3}, \tag{2}$$

where F is the buoyancy flux per unit length from a line source. For an idealized lead, $F = gQ_sW^2/U\Theta_0$ where Q_s is the upward surface temperature flux. The parameters for our case study give $[F/N^2]^{1/3} \approx 64$ m and comparison with the depth of thermal change, shown in Figure 9, indicates that the proportionality factor is approximately one. An equation for estimating the maximum plume depth, or thermal penetration downwind of a lead, is thus:

$$Z_p = \left[\frac{Q_sW^2}{U\Gamma}\right]^{1/3}, \tag{3}$$

where Γ is the environmental $\partial\theta/\partial z$ upwind of the lead. Note that the vertical extent of the plume depends strongly upon the lead width.

Equation (3) represents the vertical length scale of the atmospheric response to

a lead; it is not applicable when the wind nearly parallels the lead, i.e., when $U \approx 0$, or when the upwind atmosphere is near neutral stratification.

5.d. Recapture of heat by the ice

A portion of the upward heat flux over a lead is recaptured by the ice downwind of it, due to an increased downward heat flux there. We briefly address this question, which determines the net importance of the lead opening on the atmosphere, but the present results must be considered approximate because an LE simulation is not intended to treat surface-layer details, because the constant temperature ice surface neglects feedback effects, because the model simulation does not extend far enough downwind to cover the entire region of excess downward flux, and because radiative effects are neglected. The net heat flux is the difference between the modelled heat flux and the equilibrium surface heat flux over the ice in the absence of a lead. The net integrated heat flux over the lead is 34 Km^2/s. The heat flux downwind of the lead is initially -0.009 Km/s, decreases to -0.015 Km/s at $x = 440$ m, and then increases exponentially towards the equilibrium value of -0.0036 Km/s over an e-folding distance of 930 m, so the integrated net heat flux over the ice – estimating that beyond $x = 1000$ m by integrating the best-fit exponential – is -10 Km^2/s. Thus an estimated 30% of the surface heat input from the lead is recaptured downwind of the lead.

6. Summary and conclusions

The transfer of heat from an Arctic lead into the atmosphere has been investigated using a large-eddy (LE) simulation. The model creates individual thermal updrafts, and concomitant downdrafts, when cold Arctic air passes over a relatively warm ocean surface. The thermals grow upward until the buoyant acceleration due to their excess heat is lost, after which they decay. The integrated effect of these eddies produces a time-averaged "plume" of upward heat transport.

The vertical length scale of the atmospheric response depends upon the buoyancy flux released into the atmosphere and upon the atmospheric stratification. The relative size of two horizontal length scales, one associated with atmospheric response and the other with surface forcing, affects the qualitative nature of the turbulent field produced by the lead and the magnitude of the mean vertical velocity. For our 200 m wide lead and 2.5 m/s wind speed, the maximum response occurs downwind of the lead, not over the lead itself, because the development time of a thermal is longer than its travel time over the lead. Maximum thermal buoyancy occurs about 150 m downwind of the lead, with maximum updraft velocities – typically 28 cm/s – occurring 150 m farther downwind. Mean vertical velocities in the plume are small – typically less than 1 cm/s – as a result of updraft-downdraft compensations. The depth of the plume, and thus the depth of increased temperatures, grows downwind of the lead to reach 65 m eventually.

Since mean vertical advection is small, turbulence is primarily responsible for

the upward heat transfer. A quasi-stationary state is established with horizontal advection of relatively cold air balancing the vertical divergence of heat flux over the lead. The upward heat transfer is primarily direct, i.e., updrafts/downdrafts are relatively warm/cold. Counter-gradient heat fluxes occur at the perimeter of the plume. We believe that horizontal motion under the horizontally inhomogeneous conditions contributes to this counter-gradient heat flux and also reduces the downward heat flux at the top of the plume. A positive heat flux exists above the stably stratified layer of negative heat flux which grows downwind of the lead. Significant recapture of heat by the ice occurs downwind of the lead.

While an LE model provides an accurate simulation of convective conditions, it requires considerable computer resources so extensive examination of parameter variations is not practical. We have compared these LE results with those from a higher-order-closure (HOC) model, for identical external parameters, to test the latter's closure assumptions for an Arctic lead case and also to cross-check the LE results. The two model simulations compare favorably, so the less-computer intensive HOC model will be used to examine the effect of parameter variations upon the heat transfer; in addition, cloud and radiative effects, neglected by the LE model, will be included in the HOC simulation. We expect to present these results in a subsequent paper.

We have investigated the heat flux transferred into the atmosphere from an isolated lead, but often several leads occur in relatively close proximity. Interactions between such multiple leads may be important and we intend to investigate such effects.

Acknowledgements

We thank Chin-Hoh Moeng of the National Center for Atmospheric Research for allowing use of her LE model coding as the basis for our simulation model, as well as for answering questions about its coding. We also thank Ed Andreas of the U.S. Army's Cold Regions Research and Engineering Laboratory for his knowledgeable and detailed criticism of this work, Ron Lindsay of the Polar Science Center at the University of Washington for suggesting the importance of heat flux recapture by ice downwind of the lead, and Stuart Smith of the Bedford Institute of Oceanography for supplying smoke plume photographs of Arctic lead experiments. The authors acknowledge the support of the sponsor, Naval Oceanographic and Atmospheric Research Laboratory (NOARL) program element 61153N. This is NOARL Contribution No. 442:016:91.

References

Andreas, E. L. and Murphy, B.: 1986, 'Bulk Transfer Coefficients for Heat and Momentum over Leads and Polynyas', *J. Phys. Oceanogr.* **16**, 1875–1883.

Andreas, E. L., Paulson, C. A., Williams, R. M., Lindsay, R. W., and Businger, J. A.: 1979, 'The Turbulent Heat Flux from Arctic Leads', *Boundary-Layer Meteorol.* **17**, 57–91.

Businger, J. A., Wyngaard, J. C., Izumi, Y., and Bradley, E. F.: 1971, 'Flux Profile Relationships in the Atmospheric Surface Layer', *J. Atmos. Sci.* **28**, 181–189.

Klemp, J. B. and Durran, D. R.: 1983, 'An Upper Boundary Condition Permitting Internal Gravity Wave Radiation in Numerical Mesoscale Models', *Mon. Weather Rev.* **111**, 430–444.

Ledley, T. S.: 1988, 'A Coupled Energy Balance Climate-Sea Ice Model: Impact of Sea Ice and Leads on Climate', *J. Geophys. Res.* **93**, 15919–15932.

Lo, A. K.: 1986, 'On the Boundary-Layer Flow over a Canadian Archipelago Polynya', *Boundary-Layer Meteorol.* **35**, 53–71.

Maykut, G. A.: 1978, 'Energy Exchange over Young Sea Ice in the Central Arctic', *J. Geophys. Res.* **83**, 3646–3658.

Moeng, C.-H.: 1984, 'A Large-Eddy Simulation Model for the Study of Planetary Boundary-Layer Turbulence', *J. Atmos. Sci.* **41**, 2052–2062.

North, G. R. and Coakley, J. A.: 1979, 'Differences between Seasonal and Mean Annual Energy Balance Model Calculations of Climate and Climate Sensitivity', *J. Atmos. Sci.* **36**, 1189–1204.

Schnell, R. C., Barry, R. G., Miles, M. W., Andreas, E. L., Radke, L. F., Brock, C. A., McCormick, M. P., and Moore, J. L.: 1989, 'Lidar Detection of Leads in Arctic Sea Ice', *Nature* **339**, 530–532.

Shreffler, J. H.: 1975, 'A Numerical Model for Heat Transfer to the Atmosphere from an Arctic Lead', Ph.D. Thesis, Dept. of Oceanogr., Oregon State Univ., Corvallis, 135 pp. (Available from University Microfilms, 300 North Zeeb Road, Ann Arbor, MI 48106.)

Smith, S. D., Anderson, R. J., den Hartog, G., Topham, D. R., and Perkin, R. G.: 1983, 'An Investigation of a Polynya in the Canadian Archipelago: 2, Structure of Turbulence and Sensible Temperature', *J. Geophys. Res.* **88**, 2900–2910.

Smith, S. D., Muench, R. D., and Pease, C. H.: 1990, 'Polynyas and Leads: An Overview of Physical Processes and Environment', *J. Geophys. Res.* **95**, 9461–9479.

Turner, J. S.: 1973, *Buoyancy Effects in Fluids*, Cambridge University Press, Cambridge, 368 pp.

Untersteiner, N. (ed.): 1986, *The Geophysics of Sea Ice*, Plenum Press, N.Y., 1196 pp.

Washington, W. M. and Meehl, G. A.: 1984, 'Seasonal Cycle Experiment on the Climate Sensitivity Due to a Doubling of CO_2 with an Atmospheric General Circulation Model Coupled to a Simple Mixed-Layer Ocean Model', *J. Geophys. Res.* **89**, 9475–9503.

Wetherald, R. T. and Manabe, S.: 1981, 'Influence of Seasonal Variation upon the Sensitivity of a Model Climate', *J. Geophys. Res.* **86**, 1194–1204.

Wilczak, J. M. and Businger, J. A.: 1983, 'Thermally Indirect Motions in the Convective Atmospheric Boundary-Layer', *J. Atmos. Sci.* **40**, 343–358.